

## Effect of synthesis temperature on oxygen evolution reaction of cobalt-iron layered double hydroxide

Sung Jun Lee<sup>1</sup> · Yoo Sei Park<sup>†</sup>

(Received December 5, 2022 : Revised December 15, 2022 : Accepted December 15, 2022)

**Abstract:** Water electrolysis is a promising technology for producing renewable hydrogen energy. However, achieving high-efficiency water electrolysis has been impeded by the sluggish kinetics of the electrocatalyst. Therefore, developing highly active and cost-effective electrocatalysts for high-efficiency water electrolysis is essential. In this study, cobalt-iron layered double hydroxide (LDH) was synthesized at different temperatures using a simple co-precipitation method. Single-phase CoFe-LDH was observed only at low synthesis temperatures ( $\leq 40$  °C), and LDH and oxides existed as a mixture as the synthesis temperature increased. Further, as the synthesis temperature increased, the crystallinity and crystallite size of LDH accordingly increased. CoFe-LDH with a low crystallinity showed the best catalytic activity for the OER due to the rich crystallite boundary. This study expedites a simple and low-temperature synthesis technique of highly active OER electrocatalysts.

**Keywords:** Hydrogen energy, Oxygen evolution reaction, Electrocatalysis, Layered double hydroxide

### 1. Introduction

As a green energy carrier, hydrogen ( $H_2$ ) has several advantages, such as high energy density and clean combustion products, resulting in a wide range of applications [1]-[3]. It is considered a promising alternative to conventional fossil fuels. Among the various technologies for producing hydrogen energy, electrochemical water splitting is promising for producing renewable hydrogen energy from water. In the water-splitting reaction, the hydrogen evolution reaction (HER,  $4H_2O + 4e^- \rightarrow 4OH^- + 2H_2$ ) is a fundamental process for water-splitting because it directly generates hydrogen [4]. However, since an oxygen evolution reaction (OER,  $4OH^- \rightarrow 2H_2O + 4e^- + 2O_2$ ), which is a half-reaction in water splitting, has sluggish kinetics, the efficiency of water electrolysis is determined by the OER, and not the HER [5]. Therefore, developing highly active OER electrocatalysts is required to improve the overall efficiency of water electrolysis. Precious-metal-based electrocatalysts, e.g.,  $IrO_2$  and  $RuO_2$ , are known as the best OER electrocatalysts. However, their utilization is limited due to their high cost and scarcity [6]. Recently, transition metal-based layered double hydroxide (LDH) has emerged as the most promising electrocatalyst candidate for the OER and thus is frequently studied [7]. Particularly, Ni, Co, and

Fe-based LDHs are considered promising candidates that can have superior OER activity than precious metal-based electrocatalysts. Although LDH already has sufficient OER activity, attempts are being made to further improve its catalytic activity through control of composition, morphology engineering, and doping [8]-[10]. However, these processes have limitations in practical applications because they require multi-step and high-temperature heat treatments. Therefore, a simple and low-temperature process is necessary for practical applications.

In this study, CoFe-LDH was synthesized using a simple co-precipitation method at different temperatures and applied as an OER electrocatalyst. The synthesis temperature had a significant effect on the crystallite size of CoFe-LDH and catalytic activity for the OER. The CoFe-LDH synthesized at a low temperature showed the best OER activity with a small crystallite size.

### 2. Experimental

#### 2.1 Synthesis of CoFe

CoFe-LDH was synthesized using the co-precipitation method. First, 7 mmol cobalt(II) nitrate hexahydrate ( $Co(NO_3)_2 \cdot 6H_2O$ ) and 3 mmol iron(III) nitrate ( $Fe(NO_3)_3 \cdot 9H_2O$ ) were dissolved in deionized water (50 mL). Second, a 40 mL

<sup>†</sup> Corresponding Author (ORCID: <http://orcid.org/0000-0002-5154-2323>): Assistant Professor, Department of Advanced Material Engineering, Chungbuk National University, 1 Chungdae-ro, Seowon-gu, Cheongju-si, Chungcheongbuk-do, Korea, E-mail: [yspark@chungbuk.ac.kr](mailto:yspark@chungbuk.ac.kr), Tel: +82-43-261-2418

<sup>1</sup> Undergraduate student, Department of Advanced Material Engineering, Chungbuk National University, E-mail: [dltjdwns141@naver.com](mailto:dltjdwns141@naver.com)

This is an Open Access article distributed under the terms of the Creative Commons Attribution Non-Commercial License (<http://creativecommons.org/licenses/by-nc/3.0>), which permits unrestricted non-commercial use, distribution, and reproduction in any medium, provided the original work is properly cited.

solution containing 2 mmol potassium carbonate ( $K_2CO_3$ ) and 20 mmol potassium hydroxide (KOH) was mixed with the dissolved metal ion solution until the pH reaches 8.5. The mixture was stirred at a different temperature (20–70 °C) for 24 h, then washed. All samples were dried at 70 °C for 24 h.

## 2.2 Characterization of physical properties

X-ray diffraction (XRD) patterns were recorded using an X-ray diffractometer (D/MAX 2500, Rigaku, Tokyo, Japan) in the  $2\theta$  range of  $5^\circ$ – $80^\circ$  using Cu  $K\alpha$  radiation. The crystallite size was calculated using the Scherrer equation.

## 2.3 Electrochemical characterization

The electrochemical measurements were performed using a potentiostat (ZIVE MP1, WonATech). A three-electrode system was used for the OER, and 1M KOH solution was used as the electrolyte. A rotating disk electrode (RDE,  $0.198\text{ cm}^2$ ), and Pt-wire were used as the working electrode and counter electrode, respectively. A commercial Hg/HgO (1M KOH) was used as the reference electrode. An ink solution for the OER test was prepared by mixing the catalyst (20 mg), 5 wt.% Nafion solution (100  $\mu\text{L}$ ), and ethanol (900  $\mu\text{L}$ ). The prepared solution was sonicated for 20 min. Then, 5  $\mu\text{L}$  of the ink solution was dropped on the RDE and dried in an oven at 80 °C for 1 min. The catalytic activity for the OER was investigated by linear sweep voltammetry (LSV) at a scan rate of 5 mV/sec with 100%  $iR$ -correction. The electrochemical impedance spectroscopy (EIS) was performed at 1.63  $V_{\text{RHE}}$  and 100 kHz to 10 Hz at an amplitude of 10.0 mV. Using the Nernst equation, all the potentials were converted to a reversible hydrogen electrode (RHE,  $V_{\text{RHE}} = V$  vs. RHE) scale.

# 3. Results and discussion

## 3.1 Characterization of CoFe

CoFe were synthesized by co-precipitation at different temperatures (20–70 °C). **Figure 1(a)** shows the XRD patterns of synthesized CoFe. All the XRD patterns showed diffraction peaks at  $11.5^\circ$ ,  $23^\circ$  and  $34^\circ$  corresponding to the (003), (006), and (012) planes of the hydrotalcite-like structure, indicating the LDH structure (JCPDS:00-035-0965). The CoFe synthesized at 50 °C showed an additional diffraction peak near  $19^\circ$ , which was indexed as the (111) plane of  $Co_3O_4$  (JCPDS: 98-002-7497). In addition, this diffraction peak became sharper with increasing temperature. These results demonstrate that a temperature of 50 °C

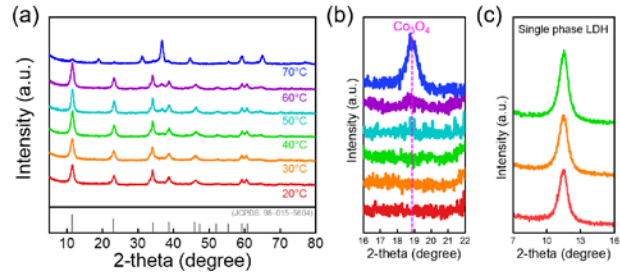


**Figure 1:** (a) XRD patterns of CoFe synthesized at different temperatures. (b) High-magnification XRD patterns ( $16^\circ < \theta < 21^\circ$ ). (c) High-magnification XRD patterns for comparison of crystallinity of single phase LDH ( $7^\circ < \theta < 16^\circ$ )

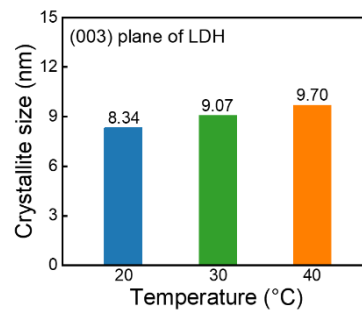


**Figure 2.** Crystallite size of CoFe synthesized at different temperatures (20, 30, and 40 °C)

or higher provided sufficient driving force to phase-transform the hydroxide phase into the oxide phase. In the single LDH phase ( $\leq 40^\circ$ ), the intensity of the peak at  $11.5^\circ$  increased as the synthesis temperature increased, indicating that the synthesis temperature affected the crystallinity of CoFe (**Figure 1(c)**) [11]. The crystallite size of CoFe was calculated using the Scherrer equation (**Figure 2**) [12]. The crystallite size decreases corresponding to the decrease in the synthesis temperature. In particular, CoFe synthesized at 20 °C has a small crystallite size of approximately 8 nm. Reducing the crystallite size widens the boundaries between crystallites, acting as defects. Consequently, the OER activity can be improved [13][14].

## 3.2 Electrochemical analysis

The OER activity of single-phase CoFe was investigated by LSV in 1 M KOH solution (**Figure 3**). In particular, the OER test was performed using CoFe synthesized at 40 °C or less to confirm the effect of temperature on the single-LDH phase. To accurately investigate the intrinsic activity of the OER, the RDE was rotated at 1600 rpm to minimize the effects of mass transfer and bubble coverage on the surface. The OER activity was compared by measuring the overpotential required to achieve a current

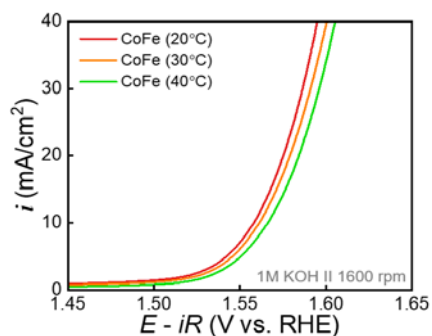


**Figure 3.** Polarization curves of CoFe synthesized at 20, 30, and 40 °C for OER.

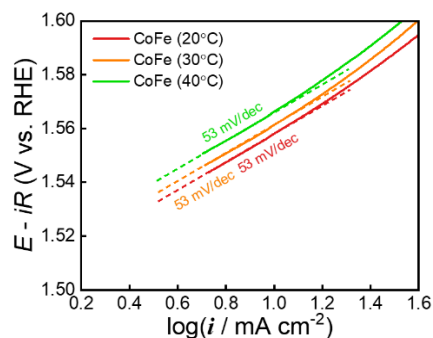


**Figure 5.** Tafel plots of CoFe synthesized at 20, 30, and 40 °C.

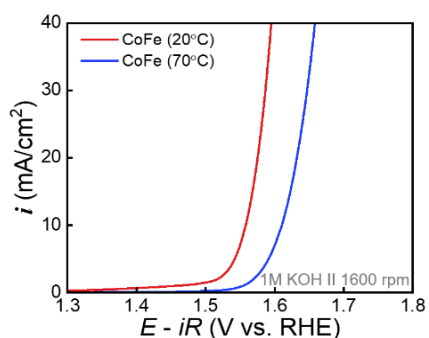


**Figure 4.** Polarization curves of CoFe (single phase) synthesized at 20 °C and CoFe (mixture of LDH and  $\text{Co}_3\text{O}_4$ ) synthesized at 70 °C for OER.

density of  $10 \text{ mA/cm}^2$ . CoFe synthesized at 20 °C showed a low overpotential of approximately 328 mV, and that synthesized at 40 °C showed a high overpotential of approximately 338 mV. An increase in overpotential was observed as the synthesis temperature increased, indicating that the OER activity of CoFe decreased with increasing synthesis temperature. Further, CoFe synthesized at 70 °C showed a high overpotential for the OER (381 mV). This is due to the reduction in LDH, the active phase of the OER, and the formation of relatively less active  $\text{Co}_3\text{O}_4$ . Tafel plots were plotted to investigate the effect of synthesis temperature on the OER kinetics mechanism of single-phase LDH (Figure 5).

The theoretical Tafel slopes for the OER are 40, 60, and 120 mV/dec. The Tafel slope of 40 mV/dec indicated that the second electron transfer was the rate-determining step (RDS), and that of 60 mV/dec indicated an  $\text{OH}^-$  intermediate coverage step after the first electron-transfer step was the RDS [15]. A Tafel slope of 120 mV/dec implies a single electron transfer step without a pre-equilibrium step. The Tafel slopes of CoFe synthesized at 20, 30, and 40 °C were  $\sim 60 \text{ mV/dec}$ , indicating the  $\text{OH}^-$  intermediate

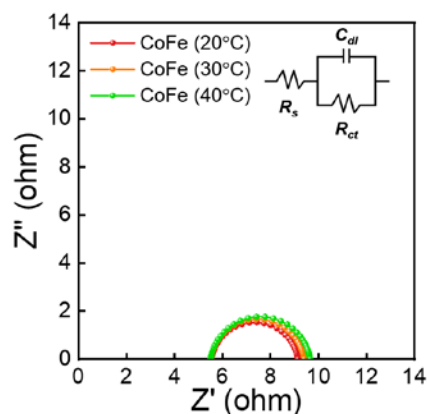


**Figure 6.** EIS of CoFe synthesized at 20, 30, 40 °C at  $1.63 \text{ V}_{\text{RHE}}$  (Randles circuit model is given in the inset).

coverage step after the first electron-transfer step was the RDS. In addition, these results indicate that the synthesis temperature did not affect the OER mechanism of CoFe. To investigate the charge transfer resistance ( $R_{ct}$ ), the EIS was performed at  $1.63 \text{ V}_{\text{RHE}}$  (Figure 6). The radius of the semi-circle implies  $R_{ct}$  for the OER. Consistent with the LSV results, the lower the synthesis temperature, the lower the  $R_{ct}$  value. In addition, the electrochemical analysis confirmed that the lower the synthesis temperature, the higher the OER activity. CoFe synthesized at a low synthesis temperature has relatively low crystallinity and rich boundaries between crystallites. Therefore, the boundaries between the crystallites acting as defects enhance the catalytic activity of the OER.

## 4. Conclusion

We investigated the effect of crystallite size on the OER by controlling the synthesis temperature of CoFe-LDH. The synthesis temperature of CoFe-LDH affected the crystallite size. The lower the synthesis temperature, the smaller the crystallite size and the richer the boundaries between crystallites that act as

defects. The CoFe-LDH synthesized at the lowest temperature had the lowest  $R_{ct}$  in the OER and consequently showed the best OER activity.

### Acknowledgements

This work was supported by the research grant of the Chungbuk National University in 2022.

### Author Contributions

Conceptualization, S. J. Lee and Y. S. Park; Methodology, S. J. Lee and Y. S. Park; Formal Analysis, S. J. Lee; Investigation, S. J. Lee; Resources, S. J. Lee and Y. S. Park; Data Curation, S. J. Lee; Writing-Original Draft Preparation, S. J. Lee; Writing-Review & Editing, Y. S. Park; Visualization, S. J. Lee; Supervision, Y. S. Park; Project Administration, Y. S. Park; Funding Acquisition, Y. S. Park.

### References

- [1] J. Yang, M. J. Jang, X. Zeng, Y. S. Park, J. Lee, S. M. Choi, *et al.*, “Non-precious electrocatalysts for oxygen evolution reaction in anion exchange membrane water electrolysis: A mini review,” *Electrochemistry Communications*, vol. 131, 2021.
- [2] M. A. Rosen, and S. Koohi-Fayeg, “The prospects for hydrogen as an energy carrier: an overview of hydrogen energy and hydrogen energy systems,” *Energy, Ecology and Environment*, vol. 1, pp. 10-29, 2016.
- [3] E. S. Bang, Y. -M. Kim, M. -H. Kim, and S. -K. Park, “Development of a 240 kW PEMFC system model for a ship,” *Journal of Advanced Marine Engineering and Technology*, vol. 44, no. 4, pp. 274-281, 2020.
- [4] Y. Zheng, Y. Jiao, A. Vasileff, and S. -Z. Qiao, “The hydrogen evolution reaction in alkaline solution: From theory, single crystal models, to practical electrocatalysts,” *Angewandte Chemie International Edition*, vol. 57, no. 26, pp. 7568-7579, 2017.
- [5] C. Kim, S. H. Kim, S. Lee, I. Kwon, S. H. Kim, S. Kim, *et al.*, “Boosting overall water splitting by incorporating sulfur into NiFe (oxy)hydroxide,” *Journal of Energy Chemistry*, vol. 64, pp. 364-371, 2022.
- [6] F. Lyu, Q. Wang, S. M. Choi, and Y. Yin, “Noble-Metal-Free electrocatalysts for oxygen evolution,” *Small*, vol. 15, no. 1, 2019.
- [7] Z. Cai, X. Bu, P. Wang, J. C. Ho, J. Yang, and X. Wang, “Recent advances in layered double hydroxide electrocatalysts for the oxygen evolution reaction,” *Journal of Materials Chemistry A*, vol. 7, pp. 5069-5089, 2019.
- [8] X. Hou, J. Li, J. Zheng, L. Li, and W. Chu, “Introducing oxygen vacancies to NiFe LDH through electrochemical reduction to promote the oxygen evolution reaction,” *Dalton Transactions*, vol. 51, pp. 13970-13977, 2022.
- [9] L. Yu, L. Wu, B. McElhenny, S. Song, D. Luo, F. Zhang, *et al.*, “Ultrafast room-temperature synthesis of porous S-doped Ni/Fe (oxy)hydroxide electrodes for oxygen evolution catalysis in seawater splitting,” *Energy & Environmental Science*, vol. 13, pp. 3439-3446, 2020.
- [10] Y. Luo, Y. Wu, D. Wu, C. Huang, D. Xiao, H. Chen, *et al.*, “NiFe-Layered double hydroxide synchronously activated by heterojunctions and vacancies for the oxygen evolution reaction,” *ACS Applied Materials & Interfaces*, vol. 12, no. 38, pp. 42850-42858.
- [11] Q. Gan, X. Cheng, J. Chen, D. Wang, B. Wang, J. Tian, *et al.*, “Temperature effect on crystallinity and chemical states of nickel hydroxide as alternative superior catalyst for urea electrooxidation,” *Electrochimica Acta*, vol. 301, pp. 47-54, 2019.
- [12] A. Monshi, M. R. Foroughi, and M. R. Monshi, “Modified Scherrer equation to estimate more accurately nano-crystallite size using XRD,” *World Journal of Nano Science and Engineering*, vol. 2, no. 3, pp. 154-160, 2012.
- [13] T. Reier, M. Oezaslan, and P. Strasser, “Electrocatalytic Oxygen Evolution Reaction (OER) on Ru, Ir, and Pt catalysts: A comparative study of nanoparticles and bulk materials,” *ACS Catalysis*, vol. 2, no. 8, pp. 1765-1772, 2012.
- [14] Q. Li, W. Mao, Y. Zhou, C. Yang, Y. Liu, and C. He, “Defects evolution and their impacts on conductivity of indium tin oxide thin films upon thermal treatment,” *Journal of Applied Physics*, vol. 118, 2015.
- [15] S. H. Kim, Y. S. Park, C. Kim, I. Y. Kwon, J. Lee, H. Jin, *et al.*, “Self-assembly of Ni-Fe layered double hydroxide at room temperature for oxygen evolution reaction,” *Energy Reports*, vol. 6, no. 7, pp. 248-254, 2020.